Prognostic validation of a neural network unified physics parameterization

N. D. Brenowitz[1]*, **C. S. Bretherton**[1]

[1]Department of Atmospheric Sciences, University of Washington

Key Points:

- A neural network based unified physics parameterization is trained on a near-global aqua-planet simulation from a cloud-resolving model.
- A numerically stable scheme is trained by minimizing the prediction error accumulated over multiple timesteps.
- Prognostic single column simulations with the neural network scheme closely match the target data.

*

Corresponding author: Noah Brenowitz, nbren12@uw.edu

Abstract

Weather and climate models approximate diabatic and sub-grid-scale processes in terms of grid-scale variables using parameterizations. Current parameterizations are designed by humans based on physical understanding, observations and process modeling. As a result, they are numerically efficient and interpretable, but potentially over-simplified. However, the advent of global high-resolution simulations and observations enables a more robust approach based on machine learning. In this letter, a neural network (NN) based parameterization is trained using a near-global aquaplanet simulation with a 4 km resolution (NG-Aqua). The NN predicts the apparent sources of heat and moisture averaged onto $(160\,\mathrm{km})^2$ grid boxes. A numerically stable scheme is obtained by minimizing the prediction error over multiple timesteps rather than single one. In prognostic single column model tests, this scheme matches both the fluctuations and equilibrium of NG-Aqua simulation better than the Community Atmosphere Model does.

1 Introduction

Numerical weather and climate models solve the primitive equations for the atmosphere at coarse resolution, and any physical processes occurring below this resolution must be parameterized [*Palmer*, 2001]. The latent heating and radiative effects of moist atmospheric convection are some of the most consequential and least well understood parameterized processes . Uncertainties in these processes likely explain the large biases in the mean state [*Hwang and Frierson*, 2013] as well as the MJO [*Jiang et al.*, 2015] and diurnal cycle [*Covey et al.*, 2016] variability of current climate models.

Traditional parameterizations are based on simplified physical models with a small number of free parameters. Cumulus parameterizations for deep convection in particular are typically based on either 1) moist convective adjustment [*Manabe and Strickler*, 1964], 2) moisture convergence closure [*Kuo*, 1974; *Tiedtke*, 1989], or 3) the quasi-equilibrium hypothesis [*Arakawa and Schubert*, 1974; *Betts*, 1986; *Betts and Miller*, 1986]. There is a long-standing debate about the validity of these hypotheses [*Emanuel et al.*, 1994; *Arakawa*, 2004], but moist convection is so complex that it is difficult to definitively prove any sort of causal relationship. Moreover, the goal of parameterization is to improve a coarse-resolution model's accuracy not to settle scientific debates.

Recent advances in cloud-resolving models (CRM)[*Bretherton and Khairoutdinov*, 2015] and observations allow a more robust approach to tuning existing parameterizations. Some recent work has proposed using ensemble Kalman filters [*Schneider et al.*, 2017] and genetic algorithms [*Langenbrunner and Neelin*, 2017] to automatically discover the parameters in a traditional parameterization. However, parameters in traditional schemes are designed to be human-interpretable rather than machine-tunable. Moreover, tuning these parameters (e.g. entrainment rates) often improves mean-state bias at the expense of degraded variability [*Kim et al.*, 2011; *Mapes and Neale*, 2011].

Machine learning (ML) techniques enable a more ambitious approach to building parameterizations based on data which do not require a human-interpretable model. ML models are more flexible than traditional parameterizations because they have thousands of free parameters, which are trained by minimizing a loss function which quantifies the error. In particular, neural networks (NN) have exploded in popularity in recent years [*Goodfellow et al.*, 2016]. In an early paper, *Krasnopolsky et al.* [2005] showed that a NN can emulate a realistic radiative transfer code but with much lower computational expense. They, then, trained a NN-based cumulus parameterization using a limited-area CRM, and showed that the scheme could accurately diagnose cloud fractions and precipitation [*Krasnopolsky et al.*, 2010, 2013]. However, a scheme which successfully predicts the instantaneous precipitation over the training data could be numerically unstable when predicting over multiple timesteps.

This letter extends *Krasnopolsky et al.* [2010, 2013] by training NN parameterizations on a near-global CRM simulation and testing the prognostic accuracy in a single column modeling framework. Single column models, which decouple the dynamics of adjacent grid cells, are commonly used to evaluate a parameterization's prognostic performance. Our biggest challenge was training a numerically stable NN-based parameterization, and our most novel contribution is introducing a new loss function that ensures long-term stability and accuracy.

Section 2 describes the near-global CRM training dataset and our coarse-graining strategy. Then, the neural network parameterization strategy is developed in Section 3. We study the prognostic performance of this scheme in Section 4 and conclude in Section 5.

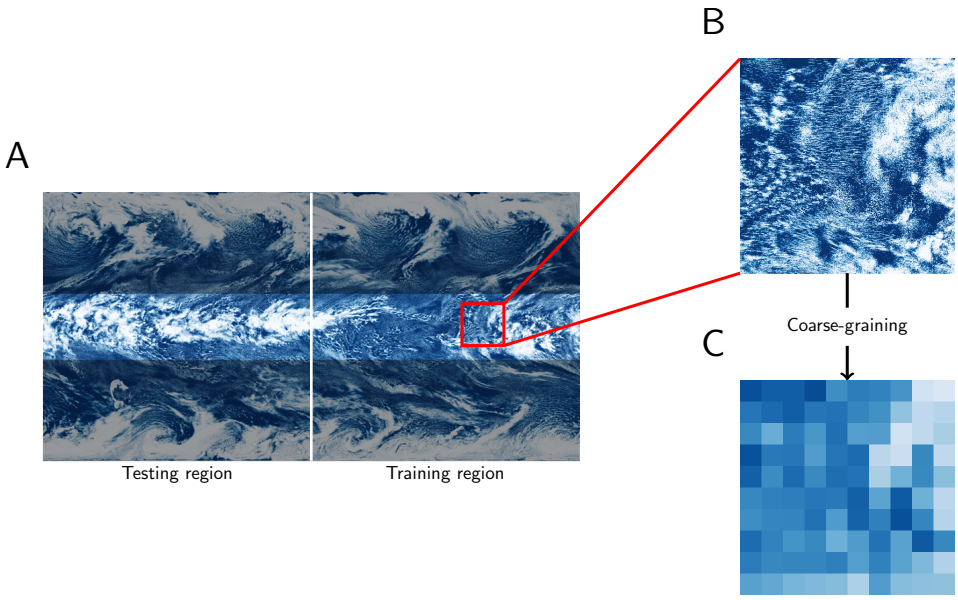

Figure 1. Schematic overview of the coarse-graining problem and the training dataset.

2 Training data and coarse-graining

2.1 Near-global Aqua-planet Simulation

The training dataset is derived from the 80-day "near-global" aqua-planet (NG-Aqua) control (CTRL) simulation described by *Narenpitak et al.* [2017] and *Bretherton and Khairoutdinov* [2015]. For NG-Aqua, the System for Atmospheric Modeling (SAM) version 6.10 *Khairoutdinov and Randall* [2003] CRM is run in a tropical channel domain 20 480 km by 10 240 km with a zonally symmetric sea surface temperature (SST) varying between 300.15 K at the equator and 278.15 K at the poleward boundaries, and a meridionally-varying Coriolis parameter. The horizontal resolution is 4 km and 3D snapshots of the prognostic variables are stored every 3 h.

The simulation uses the radiation scheme from version 3 of the Community Atmosphere Model (CAM) with a zonally uniform diurnal cycle and the original single-moment bulk microphysics scheme described by *Khairoutdinov and Randall* [2003]. SAM's prognostic thermodynamic variables are the total non-precipitating water (vapor and non-precipitating condensate) mixing ratio q_T, total precipitating water, and the liquid water/ice static temperature s_L. The mixing ratio of cloud condensate q_n is diagnosed from q_T and the absolute temperature.

The NG-Aqua control simulation has several attractive features. It has realistic multiscale organization of tropical and mid-latitude circulations, but the zonally uniform SST forces a zonally-symmetric time-mean circulation. These idealizations simplify the machine learning problem while retaining the challenge of parameterizing the effect of complex small-scale processes in a coarse-grid simulation. To further reduce the complexity , this article only uses the data lying in the tropical rain belt between $y = \pm 1280\,\mathrm{km}$. In the future, we plan to extend our approach to the extra-tropics and simulations with land regions and topography.

The large domain size and 80-day simulation length provide enough independent samples for effective training, but the 3-hour sampling interval imposes important constraints because individual convective clouds evolve on much shorter time scales. We chose to coarse-grain to $(160\,\mathrm{km})^2$ grid boxes because this size is fine enough to compare to many current climate models, but large enough that the grid box mean precipitation has a 3-hour lag correlation exceeding 0.5.

Figure 1 shows the overall schematic of the training data and coarse-graining strategy. We train and evaluate the machine learning models on the full 80 days of output from NG-Aqua. The data in the right half of the domain ($x = 10\,240\,\mathrm{km}$ to $20\,480\,\mathrm{km}$) are used for training, and the remaining data are reserved for model validation. See Table S1 for a summary of the NG-Aqua configuration.

2.2 Coarse-graining

The coarse-grained budgets for q_T and s_L are given by

$$\frac{\partial \overline{s_L}}{\partial t} + \overline{\mathbf{v}} \cdot \overline{\nabla} \overline{s}_L = Q_1 \tag{1}$$

$$\frac{\partial \overline{q_T}}{\partial t} + \overline{\mathbf{v}} \cdot \overline{\nabla} \overline{q}_T = Q_2. \tag{2}$$

Here $\overline{f}$ denotes the data averaged onto the coarse-grained grid boxes, and $\mathbf{v} = (u, v, w)$ is the three dimensional (3D) velocity. Centered differences on the coarse grid are used to estimate the 3D advection terms given by $\overline{\nabla}$. The aim of the combined atmospheric physics parameterizations in a weather forecast or climate model is to approximate the "apparent heating" Q_1 and "apparent moistening" Q_2 as functions of the coarse-grained variables alone, and thus close (1)–(2). Such a model will have interacting parameterizations for cumulus convection, radiation, boundary layer transport and other processes, some of which may have stochastic components. For this paper, we aim to machine-learn a deterministic unified

physics parameterization for their combined effects at the single coarse scale of 160 km, applied with the same 3 hour timestep of the training data. Despite these restrictions, a skillful and stable implementation would be a compelling proof of concept that can later be refined and generalized.

3 Machine learning parameterization

3.1 Model (neural network)

Like most atmospheric physics parameterizations in current large-scale models, we assume that the apparent heating and moistening only depend on data from the current grid column. Thus each grid column and time point can be considered a separate sample for training purposes. Furthermore, we assume that Q_1 and Q_2 depend on coarse-grained humidity and temperature. Because observed tropical convection is closely connected to surface fluxes, we also include the sensible (SHF) and latent (LHF) heat fluxes. We further include the insolation (SOLIN) to account for the diurnal cycle and meridional dependence of radiative heating in NG-Aqua. For simplicity, we do not include the wind profile among the predictands, nor do we predict the apparent momentum source due to parameterized physical processes.

Neural networks need normalized inputs, so we first apply some preprocessing steps to these data. First, the mean and standard deviation of the inputs are computed over the training dataset. Then, the humidity and temperature are normalized by subtracting the mean for each vertical level and dividing by the vertical average of their respective standard deviations, which are denoted by σ_q and σ_T. Because the LHF, SHF, and SOLIN are scalar, their normalization does not require vertical averaging. These normalized s_L and q_T profiles are then concatenated together to form an $2n_z$ dimensional vector for each time point t^n and coarse grained grid cell (x_i, y_i); we call this vector $\mathbf{x}_i^n$. Similarly, let $\mathbf{g}_i(t)$ be the negative of the vertically concatenated profiles of the advection terms in (1) and (2) and $\mathbf{y}_i = [\mathrm{SHF}_i^n, \mathrm{LHF}_i^n, \mathrm{SOLIN}_i^n]$.

A deterministic parameterization is a function that maps from these inputs to Q_1 and Q_2, and neural networks are powerful function approximators. While the advent of deep learning has focused on multi-layer networks, we find that single layer networks perform adequately for this task. Adding a linear function to the output of the neural network ensures that the model at least performs as well as a linear model. Thus, the NN model is a vector-valued

function $\mathbf{f}_{\text{NN}} : \mathbb{R}^{2n_z+3} \to \mathbb{R}^{2n_z}$ defined by

$$\mathbf{f}_{\text{NN}}(\mathbf{x}; \alpha) = \mathbf{W_2}\left(\mathbf{W_1}\begin{bmatrix}\mathbf{x}\\ \mathbf{y}\end{bmatrix} + \mathbf{b_1}\right)^+ + \mathbf{A}\begin{bmatrix}\mathbf{x}\\ \mathbf{y}\end{bmatrix} + \mathbf{b_2}. \tag{3}$$

The parameters for this neural network, denoted by α, are the three matrices $\mathbf{W_1}$, $\mathbf{W_2}$, and $\mathbf{A}$ in addition to the so-called bias vectors $\mathbf{b_1}$ and $\mathbf{b_2}$. Nonlinearity enters this model through the rectified linear unit (ReLU) function given by $(\cdot)^+ = \max\{0, \cdot\}$. The quantity $(\mathbf{W_1}[\mathbf{x}; \mathbf{y}] + \mathbf{b_1})^+$ is interpreted as activation of the first layer of neurons and has dimension n_{hid} which is an important hyper-parameter. The first layer is then transformed into the output space by the matrix W_2 which has dimension $2n_z \times n_{hid}$. There are $O(n_z \max\{ n_{hid}, n_z\})$ free parameters in total.

3.2 Multiple timestep loss functions

The parameters α in (3) are obtained by minimizing a loss function which quantifies the error made by a particular set of parameters. Most machine learning applications focus on specifying the right parameterization or model, and use standard notions of error such as mean-squared-error (MSE) or mean-absolute-deviation (MAD). An analogous approach for machine learning parameterization is to choose the loss function as the MSE between the neural network's predicted Q_1 and Q_2 and the discrete estimate thereof that is derived from the model output. This is the approach taken by *Krasnopolsky et al.* [2010, 2013], but they did not test their scheme in a prognostic fashion. In our own experiments, training in this fashion produces solutions that diverge to machine infinity after just a few timesteps even when the forcing is constant in time (i.e. RCE). This probably occurs because the NN-predicted Q_1 and Q_2 cause temperature and humidity errors that, although small, project onto a rapidly growing unstable mode of the neural network. Fitting $\mathbf{f}_{\text{NN}}$ to the finite difference estimate of Q_1 and Q_2 effectively minimizes the error over a single timestep and would not penalize such a mode strongly enough.

To penalize errors beyond the first timestep, the loss function should account for the mismatch between the predicted and observed time series over multiple timesteps. We therefore propose the mass-weighted loss function given by

$$J(\alpha) = \frac{1}{n_x n_y (n_t - T + 1)} \sum_i \sum_{n=1}^{n_t - T + 1} \sum_{m=0}^{T-1} ||\mathbf{x}_i^{n+m} - \mathbf{F}_\alpha^m \mathbf{x}_i^n||_W, \tag{4}$$

where the mass-weighted norm $||\cdot||_W$ is defined by

$$\left\|\begin{bmatrix}\mathbf{q}\\ \mathbf{s}\end{bmatrix}\right\| = \frac{1}{M\sigma_q}\int dz\rho_0|q(z)| + \frac{1}{M\sigma_s}\int dz\rho_0|s(z)|. \tag{5}$$

Here, $M = \int \rho_0 dz$ is the mass of an atmospheric column (i.e. surface pressure), so that J is a mass-weighted and non-dimensionalized mean-absolute deviation (MAD) error metric. In Eq. 4, n_x, n_y, and n_t are the number of zonal, meridional, and time points. The first and second summations respectively average over all horizontal locations i and valid initial time points n.

Here, the dependence of the parameters is in the operator $\mathbf{F}_\alpha^m$ which uses the NN to perform a prediction over m timesteps starting with an initial condition $\mathbf{x}$. The user-chosen hyper-parameter T controls the length of the prediction interval. The definition of $\mathbf{F}_\alpha$ is sensitive to the splitting approach used to apply the known forcings and the NN to advance the model state one timestep. *Donahue and Caldwell* [2018] show that climate models are sensitive to the order of physical parameterization. We find that applying the advection forcing and the neural network sequentially performs better than simply adding the tendencies due to the computed advection forcing and the NN. Therefore, a single timestep using the NN and the forcing is given by

$$\mathbf{x}^* = \mathbf{x} + \Delta t\frac{\mathbf{g}(t) + \mathbf{g}(t+\Delta t)}{2} \tag{6}$$

$$\mathbf{F}_\alpha\mathbf{x} = \mathbf{x}^* + \Delta t\mathbf{f}_{\mathrm{NN}}(\mathbf{x}^*;\alpha). \tag{7}$$

The m-step prediction is defined by iterating $\mathbf{F}_\alpha$ m times.

3.3 Stochastic gradient descent

The parameters α are obtained by minimizing the loss function in (4) using stochastic gradient descent [*Goodfellow et al.*, 2016, see Ch. 8]. Rather than computing the loss and its gradient over all the samples, SGD only steps down the gradient of the loss computed over a random subset of the samples, called a batch. For our purposes, a single sample is a length T sequence of the input variables $\mathbf{x}$ and the corresponding known advection forcings $\mathbf{g}$ from a single spatial location. Therefore, there are $n_x n_y(n_t - T + 1)$ total training samples. For $T = 10$, this amounts to 646144 training samples in total, which are collected into over 3000 batches of 200 each. A single pass through all the batches drawn without replacement from the entire dataset is known as an "epoch". In practice, SGD converges for our problem after 1-2 epochs, but we train the model for 5 for completeness.

The most important user-specified (i.e. hyper parameters) in our method are n_{hid}, the number of neurons in the hidden layer of the neural network, and T, the length of the interval over which the loss is evaluated (see (4)). Section 4.3 evaluates the sensitivity of the scheme to these parameters, but we use $T = 20$ and $n_{hid} = 128$ in the other sections. The computational expense scales with T, and for $T = 20$, each epoch requires approximately 5 minutes of run time on a single CPU. See Table S1 for more details about training procedure.

3.4 Prognostic validation strategy

The single column modeling (SCM) framework [*Randall et al.*, 1996] is a simple way to test our model, and is directly analogous to the training strategy described in the previous sections. An SCM evolves an initial temperature and humidity profile forward in time with prescribed advection forcing and surface fluxes. As such, it does not allow for two-way feedbacks between local physics and the environment, but it is a commonly used framework for testing parameterizations prognostically.

We compare the performance of our NN scheme to the single column version of the CAM Version 5 [*Neale et al.*, 2012]. As in the training phase, the NN prediction uses the timestepper defined in Eqs. 6 and 7 with $\Delta t = 3\,\text{h}$. The same 3D advection tendencies used to train the NN scheme are used to force CAM, and we ensure that the SOLIN matches NG-Aqua by setting the initial time to the local solar time, the latitude to $y/40\,000\,\text{km}$, and the longitude to 0°; like NG-Aqua, CAM is run in perpetual equinox mode with a circular orbit around the sun. Table S1 contains more details about the CAM configuration.

For testing, we perform an ensemble of independent single column simulations using the initial and forcing data for each horizontal grid location starting at day 0 and ending at the day 80. Because CAM is much more expensive than the neural network, we only run it for locations on the equator.

4 Results

4.1 Prognostic performance

Figure 2A,B shows the performance of the neural network (NN) and CAM when run as single column models for 80 days with observed forcing. The simulations are initialized with the NG-Aqua data for $x = 1600\,\text{km}$ and $t = 0\,\text{d}$, a point physically distant from the training region. The precipitation for the NN is computed by subtracting the mass weighted integral

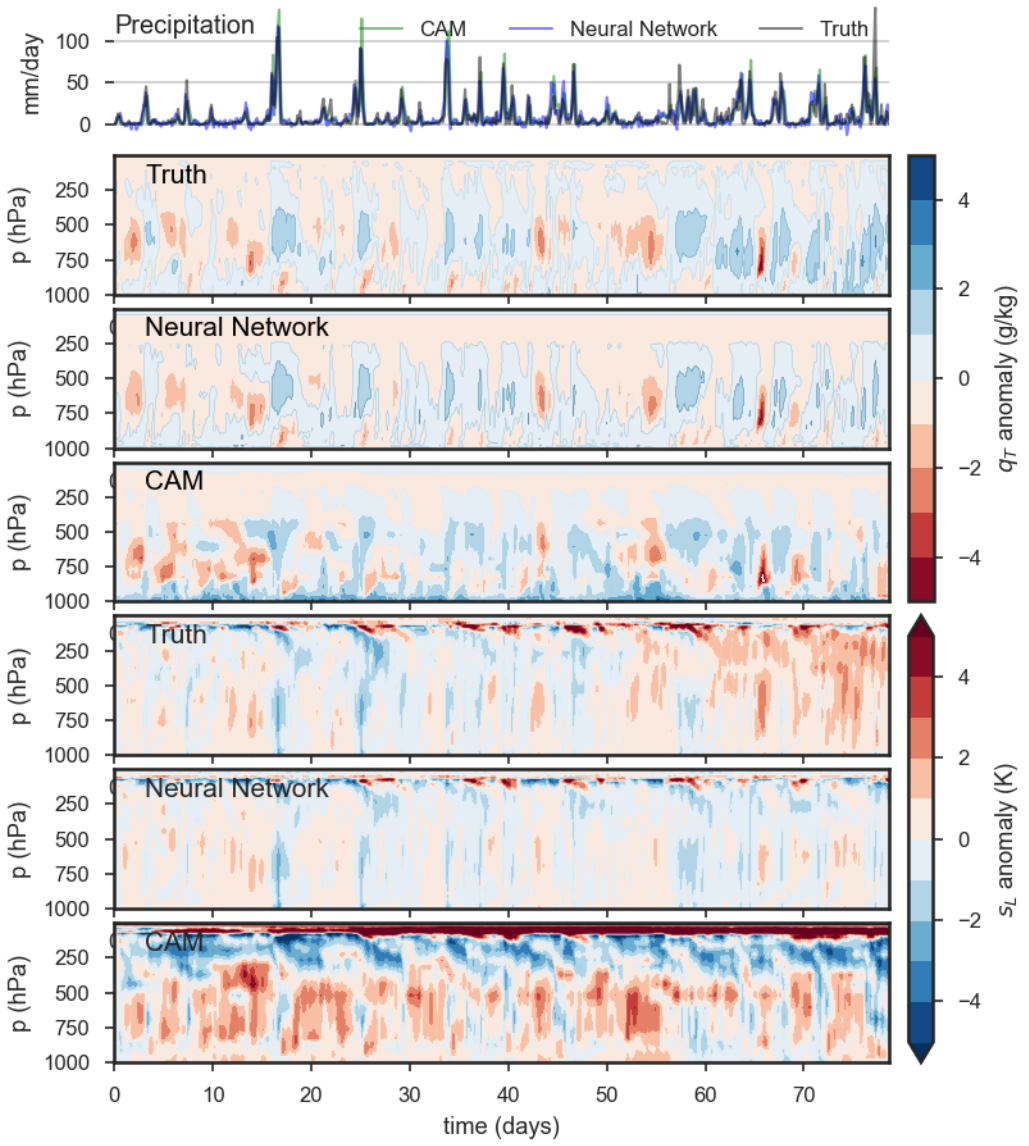

Figure 2. Forced single column model simulations comparing NG-Aqua with the predictions made by CAM and NN. The simulations are initialized with the NG-Aqua data for $(x, y, t) = (1600\,\text{km}, 0\,\text{km}, 0\,\text{d})$, and forced for all timesteps by the observed advection and surface fluxes. The precipitation is shown in the first panel. The other panels show the anomalies of q_T and s_L from the equatorial time-mean of the NG-Aqua data.

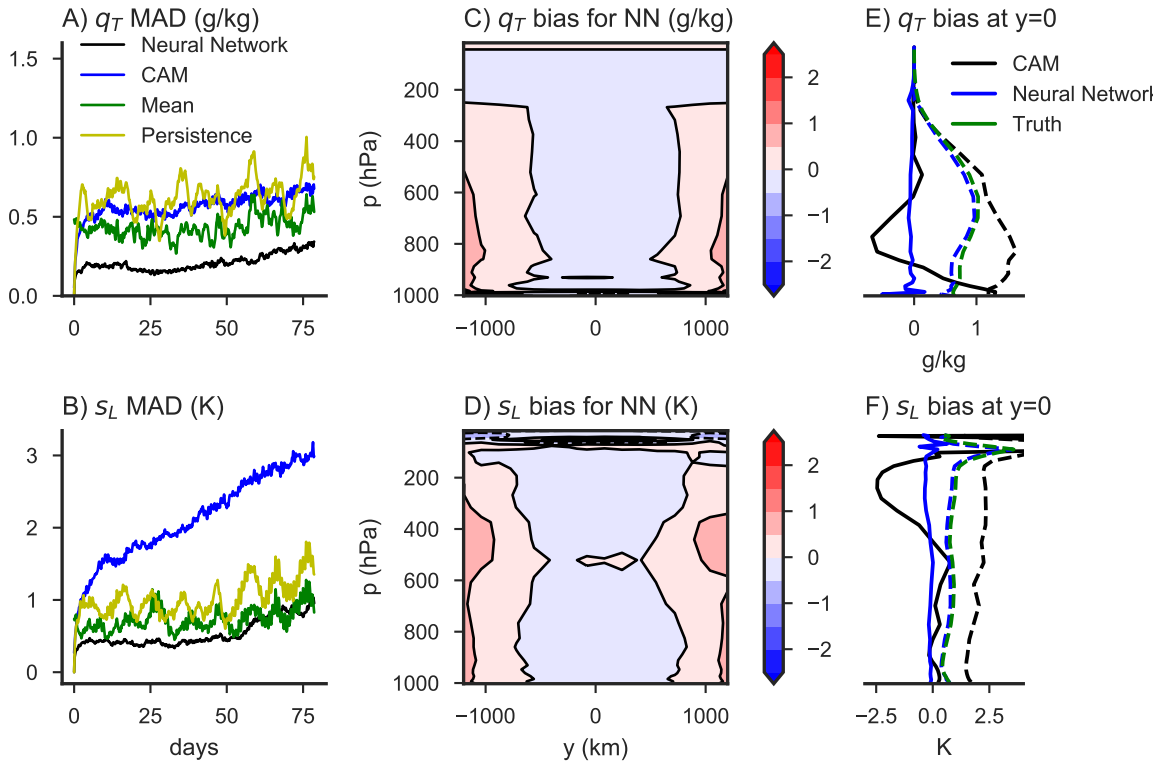

Figure 3. Humidity and temperature errors and time-mean biases. The figure shows the mass-weighted MAD error for q_T (A) and s_L (B); the zonal and time average bias for the neural network scheme for q_T (C) and s_L (D); and profiles of the mean state bias (solid) and standard deviation (dashed) for CAM and the NN scheme at $y = 0\,\text{km}$ (E and F).

of the predicted Q_2 from the evaporation [*Yanai et al.*, 1973]. Both CAM and NN capture the precipitation well, but the NN scheme does not explicitly ensure that precipitation is positive or conserves the column integrated moist static energy (cMSE). In these prognostic tests, 29% testing samples have negative precipation, accounting for -10% of the total rainfall (see Figure S1). Likewise, the mean and standard deviation of the imbalance in the cMSE budget using the true surface and top of atmosphere fluxes are $-5\,\mathrm{W\,m^{-2}}$ and $96\,\mathrm{W\,m^{-2}}$, respectively (see supplemental Text S1). On the other hand, the humidity and temperature profiles predicted by the NN much better resemble the NGAqua time series than CAM does.

The mass-weighted mean absolute deviation (MAD) over the equatorial portion of the testing region is shown in Figure 3. This is computed for s_L and q_T separately by taking a mass-weighted vertical average followed by a horizontal average over the testing region. The figure also shows the errors from a persistence forecast, which always predicts the initial data, and a time-mean forecast. The persistence forecast characterizes the auto-correlation time of the data, while the mean forecast represents the total variance of the data. The NN scheme outperforms both of these trivial forecasts for nearly all time points, especially for the q_T error, while CAM does not. CAM also produces slow temperature drifts that worsen the temperature errors at long times.

4.2 Bias

A large portion of the error made by CAM can be explained by bias. Figure 3C-E shows the bias in time and zonally averaged s_L and q_T fields produced by CAM and NN compared to the NG-Aqua data. For the locations on the equator where CAM was run, CAM has a large cold bias above 400 hPa, a moist bias in the lower troposphere, and a dry bias between 850 hPa and 600 hPa. Moreover, the standard deviation of both q_T and s_L is too large for all heights. On the other hand, NN has almost no bias along the equator and the standard deviation closely matches the NG-Aqua data. The bias made by the NN scheme increases away from the equator to a maximum temperature (humidity) bias of less than 1 K and $1\,\mathrm{g\,kg^{-1}}$. This bias probably occurs towards the northern/southern boundaries of the training region because most of the training data is closer to the equator. Nonetheless, this bias is quite small considering that the climatological precipitation varies from $2\,\mathrm{mm\,d^{-1}}$ to $10\,\mathrm{mm\,d^{-1}}$ over this region, which shows that the NN scheme performs well in a variety of environments.

Table 1. Performance for different hyper-parameters. For each parameter set, we train an ensemble of 5 neural networks and show the median score. The R^2 scores are dimensionless. The 64-step MAD scores for q_T and s_L have units g kg^{-1} and K, respectively. The parenthesis shows the uncertainty of the median score, which is defined as half the distance between the maximum and minimum scores over 200 bootstrapped samples.

n_{hid}	T	Apparent Source R^2		64-step MAD	
		q_T	s_L	q_T (g kg^{-1})	s_L (K)
5	10	0.55 (0.03)	0.70 (0.05)	0.79 (0.18)	1.35 (0.28)
64	10	0.60 (0.03)	0.73 (0.05)	0.45 (0.06)	0.79 (0.08)
128	10	0.59 (0.02)	0.73 (0.05)	0.37 (0.03)	0.63 (0.02)
256	10	0.59 (0.03)	0.73 (0.05)	0.33 (0.03)	0.62 (0.04)
128	2	0.63 (0.02)	0.74 (0.04)	1.23 (1.20)	2.24 (2.62)
128	5	0.62 (0.03)	0.74 (0.05)	0.58 (0.13)	1.05 (0.19)
128	10	0.59 (0.02)	0.73 (0.05)	0.37 (0.03)	0.63 (0.02)
128	20	0.55 (0.03)	0.72 (0.05)	0.27 (0.01)	0.54 (0.01)
128	40	0.27 (0.08)	0.46 (0.09)	0.30 (0.04)	0.57 (0.03)

4.3 Sensitivity to hyper-parameters

We now analyze the sensitivity to the two main hyper-parameters in our method: the training window size (T) and the number of hidden neurons (n_{hid}). Each parameter set is evaluated by two error metrics for each variable. The first metric is the mass-weighted coefficient of determination (R^2) between the Q_1 and Q_2 estimated from NG-Aqua directly using finite differences in space and time, and those predicted by the NN. The second metric is the cumulative mean absolute deviation (MAD) of a 64 step (8 day) forecast using the NN. Because training a NN is a stochastic process, we generate an ensemble of 5 NN models for each hyper-parameter set by changing the seed of the pseudo-random number generator.

Table 1 shows these error metrics for increasing n_{hid} with fixed $T = 10$ and for increasing T with fixed $n_{hid} = 128$. For fixed T, increasing the number of hidden neurons hardly improves the R^2 scores for the apparent heat sources. Even networks with $n_{hid} = 5$ can explain 60% and 70% of the variance of the apparent sinks of moisture and temperature, respectively, as also found by *Krasnopolsky et al.* [2013]. On the other hand, $n_{hid} = 5$ makes

more than twice as much error in the 64-step prediction than $n_{hid} = 128$ does. These results confirm that just fitting the apparent source does not ensure long-term accuracy, which requires using more neurons that *Krasnopolsky et al.* [2013] suggest.

For a fixed number of hidden nodes, there is a trade-off between 64-step MAD and apparent source R^2. Longer window sizes show better (worse) performance on the 64-step MAD (apparent source R^2), which is not surprising because the apparent source R^2 is closely related to the 1-step error. That said, increasing the window size from 2 to 20 minimally degrades the apparent source R^2 scores, but dramatically improves the 64-step MAD. Moreover, the 64-step MAD under-represents the errors of the $T = 2$ schemes, which eventually diverge to machine infinity after approximately 20 days of simulation.

5 Discussion and Conclusion

In this study, we used the tropical region of a near-global cloud resolving model to train a unified physics parameterization based on neural networks. A feed-forward neural network was trained to predict the residual source terms of the total water and liquid water static energy coarse-grained onto $(160\,\mathrm{km})^2$ grid boxes. As such, it accounts for the effect of radiation, cumulus convection, and any other physics beyond grid-scale advection on the coarse grid.

The parameters of this neural network are trained by stochastic gradient descent of a loss function. Choosing an appropriate loss function is the key to training a neural network parameterization that is numerically stable and accurate over many timesteps. Past studies trained their models to minimize the error between the neural network outputs and the apparent heating and moistening computed by subtracting one timestep from the next. This approach is equivalent to minimizing the prediction error over a single timestep, which we find invariably produces a numerically unstable parameterization. By minimizing the accumulated error over several days of prediction, we can successfully train a neural network which is numerically stable.

This neural network matches the NG-Aqua simulation substantially better than the Community Atmosphere Model (CAM) does in 80-day single column tests with specified advection forcings and surface fluxes, and no relaxation toward the "truth" profiles. CAM responds to this forcing too strongly, has a mean drift in humidity, and larger variations in temperature and humidity than were simulated by the cloud-resolving model. On the other

hand, the predicted mean, variance, and time-dependent behavior of the neural network scheme closely match the data. That said, CAM, unlike the NN, was not specifically tuned to match the statistics of the NG-Aqua simulation. Moreover, the NG-Aqua simulation certainly contains its own biases with respect to observations and higher resolution models. While small overall, the bias of the neural network scheme increases towards the poleward boundaries of the training region. The neural network is moderately expensive to train, but runs faster than the single-column CAM because it is simpler and uses a longer timestep.

Since the neural network scheme performs well on single column tests, the next step is to couple it to the dynamical core of a coarse resolution three-dimensional atmospheric model. Beyond this, it is natural to extend analogous methodology to regions outside the deep tropics and over land with complex terrain and coastlines. A realistic parameterization should also predict the coarse-grained sub-grid momentum flux profiles in regions of convection and flow over complex terrain for parameterization of atmospheric drag and gravity-wave breaking. Moist atmospheric convection is an inherently stochastic process, so neural networks should generate coarse-grained outputs whose randomness is trained to match that of their training datasets. While we trained a unified physics parameterization, there are conceptual reasons why separate physical processes such as microphysics, radiation, and sub-grid-scale transport should be separately parameterized, potentially with a mixture of machine learning and conventional approaches. Likewise, a neural network scheme should also satisfy basic physical constraints such as moist static energy conservation and the positivity of precipitation. Finally, high-resolution models are also imperfect, so methods for incorporating observations and data assimilation into the training methodology will be needed.

Acknowledgments

N.B. is supported as a postdoctoral fellow by the Washington Research Foundation, and by a Data Science Environments project award from the Gordon and Betty Moore Foundation (Award #2013-10-29) and the Alfred P. Sloan Foundation (Award #3835) to the University of Washington eScience Institute. C.B. is supported by U. S. Department of Energy grants DE-SC0012451 and DE-SC00164. We thank Aleksandr Aravkin and Nathan Kutz for helpful discussions regarding multiple timestep loss functions, and an anonymous reviewer for their constructive comments. The coarse-grained NG-Aqua data and computer codes used here are available on `zenodo.org` [*Brenowitz*, 2018a] and `github.com` [*Brenowitz*, 2018b], respectively.

References

Arakawa, A. (2004), The cumulus parameterization problem: Past, present, and future, *J. Clim.*, *17*(13), 2493–2525, doi:10.1175/1520-0442(2004)017<2493:RATCPP>2.0.CO;2.

Arakawa, A., and W. H. Schubert (1974), Interaction of a cumulus cloud ensemble with the Large-Scale environment, part I, *J. Atmos. Sci.*, *31*(3), 674–701, doi:10.1175/1520-0469(1974)031<0674:IOACCE>2.0.CO;2.

Betts, A. K. (1986), A new convective adjustment scheme. part i: Observational and theoretical basis, *Q.J.R. Meteorol. Soc.*, *112*(473), 677–691, doi:10.1002/qj.49711247307.

Betts, A. K., and M. J. Miller (1986), A new convective adjustment scheme. part II: Single column tests using GATE wave, BOMEX, ATEX and arctic air-mass data sets, *Q.J.R. Meteorol. Soc.*, *112*(473), 693–709, doi:10.1002/qj.49711247308.

Brenowitz, N. D. (2018a), Coarse-grained outputs from near-global aqua-planet control run with qobs sst, doi:10.5281/zenodo.1226370.

Brenowitz, N. D. (2018b), `nbren12/nn_atmos_param v0.3`, doi:10.5281/zenodo.1228392.

Bretherton, C. S., and M. F. Khairoutdinov (2015), Convective self-aggregation feedbacks in near-global cloud-resolving simulations of an aquaplanet, *Journal of Advances in Modeling Earth Systems*, *7*(4), 1765–1787.

Covey, C., P. J. Gleckler, C. Doutriaux, D. N. Williams, A. Dai, J. Fasullo, K. Trenberth, and A. Berg (2016), Metrics for the diurnal cycle of precipitation: Toward routine benchmarks for climate models, *J. Clim.*, *29*(12), 4461–4471, doi:10.1175/JCLI-D-15-0664.1.

Donahue, A. S., and P. M. Caldwell (2018), Impact of physics parameterization ordering in a global atmosphere model, *J. Adv. Model. Earth Syst.*, *10*(2), 481–499, doi:10.1002/2017MS001067.

Emanuel, K. A., J. David Neelin, and C. S. Bretherton (1994), On large-scale circulations in convecting atmospheres, *Q.J.R. Meteorol. Soc.*, *120*(519), 1111–1143, doi:10.1002/qj.49712051902.

Goodfellow, I., Y. Bengio, and A. Courville (2016), *Deep learning*, Adaptive computation and machine learning, The MIT Press, Cambridge, Massachusetts.

Hwang, Y.-T., and D. M. W. Frierson (2013), Link between the double-intertropical convergence zone problem and cloud biases over the southern ocean, *Proc. Natl. Acad. Sci. U. S. A.*, *110*(13), 4935–4940, doi:10.1073/pnas.1213302110.

Jiang, X., D. E. Waliser, P. K. Xavier, J. Petch, N. P. Klingaman, S. J. Woolnough, B. Guan, G. Bellon, T. Crueger, C. DeMott, C. Hannay, H. Lin, W. Hu, D. Kim, C.-L. Lappen, M.-M. Lu, H.-Y. Ma, T. Miyakawa, J. A. Ridout, S. D. Schubert, J. Scinocca, K.-H. Seo, E. Shindo, X. Song, C. Stan, W.-L. Tseng, W. Wang, T. Wu, X. Wu, K. Wyser, G. J. Zhang, and H. Zhu (2015), Vertical structure and physical processes of the Madden-Julian oscillation: Exploring key model physics in climate simulations, *J. Geophys. Res. D: Atmos.*, *120*(10), 2014JD022,375, doi:10.1002/2014JD022375.

Khairoutdinov, M. F., and D. A. Randall (2003), Cloud resolving modeling of the ARM summer 1997 IOP: Model formulation, results, uncertainties, and sensitivities, *J. Atmos. Sci.*, *60*(4), 607–625, doi:10.1175/1520-0469(2003)060<0607:CRMOTA>2.0.CO;2.

Kim, D., Y.-S. Jang, D.-H. Kim, Y.-H. Kim, M. Watanabe, F.-F. Jin, and J.-S. Kug (2011), El niño-southern oscillation sensitivity to cumulus entrainment in a coupled general circulation model: ENSO SENSITIVE TO CONVECTION SCHEME, *J. Geophys. Res.*, *116*(D22), doi:10.1029/2011JD016526.

Krasnopolsky, V. M., M. S. Fox-Rabinovitz, and D. V. Chalikov (2005), New approach to calculation of atmospheric model physics: Accurate and fast neural network emulation of longwave radiation in a climate model, *Mon. Weather Rev.*, *133*(5), 1370–1383, doi:10.1175/MWR2923.1.

Krasnopolsky, V. M., M. S. Fox-Rabinovitz, and A. A. Belochitski (2010), Development of neural network convection parameterizations for numerical climate and weather prediction models using cloud resolving model simulations, in *The 2010 International Joint Conference on Neural Networks (IJCNN)*, pp. 1–8, doi:10.1109/IJCNN.2010.5596766.

Krasnopolsky, V. M., M. S. Fox-Rabinovitz, and A. A. Belochitski (2013), Using ensemble of neural networks to learn stochastic convection parameterizations for climate and numerical weather prediction models from data simulated by a cloud resolving model, *Advances in Artificial Neural Systems*, *2013*, e485,913, doi:10.1155/2013/485913.

Kuo, H. L. (1974), Further studies of the parameterization of the influence of cumulus convection on Large-Scale flow, *J. Atmos. Sci.*, *31*(5), 1232–1240, doi:10.1175/1520-0469(1974)031<1232:FSOTPO>2.0.CO;2.

Langenbrunner, B., and J. D. Neelin (2017), Pareto-Optimal estimates of california precipitation change, *Geophys. Res. Lett.*, p. 2017GL075226, doi:10.1002/2017GL075226.

Manabe, S., and R. F. Strickler (1964), Thermal equilibrium of the atmosphere with a convective adjustment, *J. Atmos. Sci.*, *21*(4), 361–385, doi:10.1175/1520-

0469(1964)021<0361:TEOTAW>2.0.CO;2.

Mapes, B., and R. Neale (2011), Parameterizing convective organization to escape the entrainment dilemma, *J. Adv. Model. Earth Syst.*, *3*(2), M06,004, doi:10.1029/2011MS000042.

Narenpitak, P., C. S. Bretherton, and M. F. Khairoutdinov (2017), Cloud and circulation feedbacks in a near-global aquaplanet cloud-resolving model: Cloud feedbacks in a Near-Global CRM, *J. Adv. Model. Earth Syst.*, *9*(2), 1069–1090, doi:10.1002/2016MS000872.

Neale, R. B., C.-C. Chen, A. Gettelman, P. H. Lauritzen, S. Park, D. L. Williamson, A. J. Conley, R. Garcia, D. Kinnison, J.-F. Lamarque, and Others (2012), Description of the NCAR community atmosphere model (CAM 5.0), *NCAR Tech. Note NCAR/TN-486+ STR*, *1*(1), 1–12.

Palmer, T. N. (2001), A nonlinear dynamical perspective on model error: A proposal for non-local stochastic-dynamic parametrization in weather and climate prediction models, *Quart. J. Roy. Meteor. Soc.*, *127*(572), 279–304, doi:10.1002/qj.49712757202.

Randall, D. A., K.-M. Xu, R. J. C. Somerville, and S. Iacobellis (1996), Single-Column models and cloud ensemble models as links between observations and climate models, *J. Clim.*, *9*(8), 1683–1697, doi:10.1175/1520-0442(1996)009<1683:SCMACE>2.0.CO;2.

Schneider, T., S. Lan, A. Stuart, and J. Teixeira (2017), Earth system modeling 2.0: A blueprint for models that learn from observations and targeted High-Resolution simulations, *Geophys. Res. Lett.*, *44*(24), 12,396–12,417, doi:10.1002/2017GL076101.

Tiedtke, M. (1989), A comprehensive mass flux scheme for cumulus parameterization in Large-Scale models, *Mon. Weather Rev.*, *117*(8), 1779–1800, doi:10.1175/1520-0493(1989)117<1779:ACMFSF>2.0.CO;2.

Yanai, M., S. Esbensen, and J.-H. Chu (1973), Determination of bulk properties of tropical cloud clusters from Large-Scale heat and moisture budgets, *J. Atmos. Sci.*, *30*(4), 611–627, doi:10.1175/1520-0469(1973)030<0611:DOBPOT>2.0.CO;2.